

## Universal Defects Statistics with Strong Long-Range Interactions

Stefano Gherardini<sup>1,2</sup>, Lorenzo Buffoni<sup>3</sup>, and Nicolò Defenu<sup>4,5</sup>


<sup>1</sup>*CNR-INO, Largo Enrico Fermi 6, I-50125 Firenze, Italy*

<sup>2</sup>*LENS, Università di Firenze, I-50019 Sesto Fiorentino, Italy*

<sup>3</sup>*Department of Physics and Astronomy, University of Florence, 50019 Sesto Fiorentino, Italy*

<sup>4</sup>*Institut für Theoretische Physik, ETH Zürich, Wolfgang-Pauli-Strasse 27 Zürich, Switzerland*

<sup>5</sup>*CNR-INO, Area Science Park, Basovizza, I-34149 Trieste, Italy*

 (Received 9 June 2023; revised 23 February 2024; accepted 10 July 2024; published 11 September 2024)

Quasi-static transformations, or slow quenches, of many-body quantum systems across quantum critical points generate topological defects. The Kibble-Zurek mechanism regulates the appearance of defects in a local quantum system through a classical combinatorial process. However, long-range interactions disrupt the conventional Kibble-Zurek scaling and lead to a density of defects that is independent of the rate of the transformation. In this Letter, we analytically determine the complete full counting statistics of defects generated by slow annealing a strong long-range system across its quantum critical point. We demonstrate that the mechanism of defect generation in long-range systems is a purely quantum process with no classical equivalent. Furthermore, universality is not only observed in the defect density but also in all the moments of the distribution. Our findings can be tested on various experimental platforms, including Rydberg gases and trapped ions.

DOI: [10.1103/PhysRevLett.133.113401](https://doi.org/10.1103/PhysRevLett.133.113401)

*Introduction*—Universal dynamical scaling is often encountered in many-body systems driven across an equilibrium critical point. Signatures of dynamical universality in classical systems date back to the seminal observations of Kibble and Zurek on the scaling of the density of defects generated by the quasi-static transformation of a many-body Hamiltonian across its critical point [1,2]. Since these early studies, many experimental evidences of the Kibble-Zurek mechanism (KZM) have been attained [3–6], making it probably the most accessible example of dynamical universality in modern physics [7]. Because of quantum-classical correspondence, the KZM shall also apply to slow unitary dynamics across a quantum critical point (QCP). The applicability of KZM to the scaling of topological defects at zero temperatures was first conjectured by finite size scaling arguments [8] and, then, demonstrated exactly on the nearest-neighbor Ising model [9]. Several following studies evidenced the universality of the KZM picture and the ubiquity of its applicability; see Ref. [5] for a review.

The KZM predicts that the average number of defects scales with the quench time  $\tau$  following a universal power-law scaling. The same scaling describes the density of

excitations in the quantum domain as well. It has been recently argued that, given a system whose critical dynamics is described by the KZM, the full number distribution of topological defects is universal and described by a binomial distribution [10–13]. In this picture, the formation of each topological defect is an independent random process over time and, denoting with  $L$  the total number of merging points, the probability  $p(\ell)$  for the formation of  $\ell$  defects in spin or fermionic systems is

$$p(\ell) \sim \text{B}(\ell, L, q) = \binom{L}{\ell} q^\ell (1-q)^{L-\ell}, \quad (1)$$

where  $1-q$  is the probability that no defect is originated. In probability theory, this law describes the number of successes in a sequence of independent Bernoulli trials, as, e.g., a coin toss [14]. It is worth noting that the coherent quantum dynamics do not actually impact the distribution of topological defects in the local case, which indeed corresponds to the one of a classical process [14]. In fact, the KZM can be deduced by purely adiabatic arguments, which involve only the equilibrium scaling exponents; see Sec. 2.3 in Ref. [5]. The equilibrium scaling exponents can, in turns, be related to the classical picture via the celebrated quantum-to-classical correspondence [15]. The previous result can be neatly extended to the entire defect distribution, as it is shown by the correspondence between the classical numerical study of Ref. [11] and the exact calculation for the transverse field quantum Ising chain [10]. On the contrary, the formation of defects in

---

*Published by the American Physical Society under the terms of the Creative Commons Attribution 4.0 International license. Further distribution of this work must maintain attribution to the author(s) and the published article's title, journal citation, and DOI.*

long-range (LR) systems does not follow the traditional KZM picture [16,17] and the full counting defect statistics of the quantum LR ferromagnetic Ising model appear to be a distinctive consequence of the coherent quantum dynamics.

In fact, while power-law decaying interactions  $\propto r^{-\alpha}$  with  $\alpha < d$  induce semiclassical universal scaling at equilibrium, in the out-of-equilibrium regime they allow to circumvent the constraints imposed by decoherence and equilibration, often enhancing quantum effects [18]. The prominent collective character of the LR systems generates a kaleidoscope of novel phenomena, including supersonic propagation of correlations [19–21], fast entanglement spreading and shielding [22–26], and anomalous scaling dynamics and ergodicity breaking [27–29]. It is worth noting that most of these results have been obtained in systems of Fermi quasiparticles, which are also at the basis of our current understanding of the KZM [9,30–33]. On the contrary, the following picture will focus on systems, whose effective low-energy theory features Bose quasiparticles.

*The model*—We are going to consider the full counting statistics of topological defects generated by a slow quench across the QCP of the Ising model with flat fully connected interactions. This model follows the Lipkin-Meshkov-Glick (LMG) Hamiltonian [34–36], which is one of the landmarks of quantum annealing [37],

$$H_{\text{LMG}} = -J \left( \sum_{i < j} \sigma_i^x \sigma_j^x + (\lambda(t/\tau) + 1) \sum_i \sigma_i^z \right), \quad (2)$$

where  $J$  denotes the interaction strength (constant energy shift), and  $\lambda$  is the time-dependent deviation of the magnetic field from unity, corresponding to the QCP of the model, with  $t \in [-\tau, \tau]$ . The indexes  $i, j$  run over all  $N$  sites of a one-dimensional lattice. For any slow quench terminating at or across the QCP, universal scaling of the defects statistics is expected to appear. In the following, we will determine the full counting statistics  $\mathcal{P}(m)$  of topological defects generated by this annealing protocol, demonstrating that  $\mathcal{P}(m)$  follows a *negative binomial distribution*. Contrarily to the binomial distribution in Eq. (1), a negative binomial distribution assigns a probability weight to the number of failures  $m$  that occur in a sequence of independent Bernoulli trials before  $r$  successes are observed. In our case, the event denoted as “failure” is the formation of a topological defect and occurs with finite probability.

The peculiarity of the LR phenomenology descends from *not* having an integer value for the number of successes (i.e.,  $r \in \mathbb{R}$ ), which reflects the fact that an infinitely degenerate QCP is considered. Because of the degeneracy of the QCP, the number of topological defects can be unbounded, and, in principle, a negative binomial distribution with fractional index may be predicted by any bosonic theory with gapped quasiparticle spectrum in the low-energy approximation. For these reasons, since a

negative binomial distribution with fractional index is not linked to any classical combinatorial problem, the process of defects formation in the quantum LR Ising model does not have a classical counterpart. This has to be compared with the case of the nearest-neighbor quantum Ising model, where the classical analogy is straightforward [14].

*Effective low-energy theory*—The construction of the effective low-energy theory follows the same line as in Ref. [17]. We introduce the leading order Holstein-Primakov approximation [38] of the total spin operator  $S = \sum_i \sigma_i$  with  $\sigma_i = (\sigma_i^x, \sigma_i^y, \sigma_i^z)$ . At equilibrium, this approach reduces the total spin components to position  $x$  and momentum  $p$  coordinates, i.e.,  $S_z = N/2 - (x^2 + p^2 - 1)/2$ ,  $S_x = \sqrt{N/2}x$  and  $S_y = \sqrt{N/2}p$ , where operators  $x$  and  $p$  satisfy the bosonic commutation relation  $[x, p] = i\hbar$ . It is evident that the aforementioned approximation will remain sensible as long as the system remains close to the full paramagnetic state  $\langle S_z \rangle / N \approx -1/2$ . This condition is naturally violated during a quasistatic dynamics crossing the QCP. We generalize the procedure in the out-of-equilibrium regime, by aligning the axis of  $S_z$  with the direction of the instantaneous magnetization; see Refs. [39,40]. Assuming that the classical variable describing the instantaneous magnetization adiabatically follows the quasistatic drive, the leading source of deviations from adiabaticity emerges from quantum (energy) fluctuations. The latter are described by the Hamiltonian

$$\mathcal{H}_t = \frac{p^2}{2M} + \frac{M}{2} \omega_t^2 x^2, \quad (3)$$

which is obtained from Eq. (2) by introducing the Holstein-Primakov relations [41]. In Eq. (3),  $M$  is the mass of the oscillator and  $\omega_t$  denotes the time-dependent driving function. As the system approaches the QCP, quantum fluctuations become soft and, accordingly, the frequency follows  $\omega_t \sim \sqrt{\lambda(t/\tau)}$ . In order to include effects caused by finite system sizes or small magnetic fields, we will also consider the case of imperfect crossings, i.e.,  $\lim_{t \rightarrow 0} \omega_t = \omega_c \gtrsim 0$  with  $t = 0$  being the time when the crossing occurs.

In choosing the time behavior of  $\omega_t$ , we reproduce the standard Kibble-Zurek protocol [50]: at  $t = \tau$  the system is prepared in the ground state of  $\mathcal{H}_\tau$  with a regular and well-separated spectrum ( $\omega_\tau \gg 0$ ). Then, the quantum system is driven in order to reduce the spectral gap until the instantaneous spectrum becomes fully degenerate (or nearly so for  $\omega_c \gtrsim 0$ ). As customary [5], we only consider the leading order of the drive in the vicinity of the QCP, so that the time-dependent frequency takes the form  $\omega_t^2 \sim |t/\tau|^\eta$ , where  $\eta$  denotes a scaling exponent. Beyond the QCP at  $t > 0$ , the energy gap opens up again until the dynamic terminates at  $t = \tau$ .

*Average energy and defects formation*—The driving function  $\omega_t$  entails time-dependent variations of the internal

energy  $\Delta E_t$  of the system. Classically, at any time  $t$ , the internal energy is a stochastic variable defined as  $\Delta E_t = E_t^{(m)} - E_{t_0}^{(n)}$ , where  $\{E^{(n)}\}$  and  $\{E^{(m)}\}$  are the set of eigenvalues of  $\mathcal{H}_{t_0}$  and  $\mathcal{H}_t$ , respectively. The latter are formally provided by expressing the Hamiltonian (3) at  $t_0$  and  $t$  in spectral representation, i.e.,

$$\mathcal{H}_{t_0} = \sum_n E_{t_0}^{(n)} \Pi_{t_0}^{(n)} \quad \text{and} \quad \mathcal{H}_t = \sum_m E_t^{(m)} \Pi_t^{(m)}, \quad (4)$$

where  $\Pi_{t_0}^{(n)} = |\phi_{t_0}^{(n)}\rangle\langle\phi_{t_0}^{(n)}|$  and  $\Pi_t^{(m)} = |\phi_t^{(m)}\rangle\langle\phi_t^{(m)}|$  are the projectors on the instantaneous energy eigenstates. Thus,  $|\phi_t^{(\ell)}\rangle$  denotes the  $\ell$ th eigenfunction of  $\mathcal{H}_t$ , with  $\ell \in \{n, m\}$  unbounded (from above) integer number. Instead, the instantaneous energy values  $E_t^{(\ell)}$  are equal to  $E_t^{(\ell)} = \hbar\omega_t(\ell + \frac{1}{2})$ , with  $\hbar$  reduced Planck constant.

The corresponding average internal energy  $\langle\Delta E_t\rangle$ , which is the expected value of the distribution of  $\Delta E_t$ , can be interpreted as the average *reversible* quantum (stochastic) work  $\langle W \rangle$  provided the driving function is an *adiabatic* transformation [51]. This means that, in case the drive is not adiabatic, part of the internal energy  $\Delta E$  cannot be converted in useful work. Hence, from the first law of thermodynamics  $\langle\Delta E_t\rangle = \langle W \rangle_{\text{rev}} + \langle W \rangle_{\text{irr}}$ , in our setting  $\langle W \rangle_{\text{irr}} \approx 0$  for  $t < 0$ . Instead, the system dynamics becomes irreversible from crossing the QCP, and the amount of irreversible work decreases for higher values of  $\omega_C$ . In fact, the average internal energy  $\Delta E_t$  can be decomposed as

$$\langle\Delta E_t\rangle = \frac{\hbar}{2}(\omega_t - \omega_{t_0}) + \hbar\omega_t\langle\nu_t\rangle, \quad (5)$$

where the first term on the rhs represents the adiabatic correction  $\langle W \rangle_{\text{rev}}$  to the quantum work, while the second term  $\hbar\omega_t\langle\nu_t\rangle$  is the nonadiabatic contribution, i.e., the irreversible work  $\langle W \rangle_{\text{irr}}$ . The latter is proportional to the average number of excitations (or defects density)  $\langle\nu_t\rangle = \sum_m \langle\psi_t|m\Pi_t^{(m)}|\psi_t\rangle$  generated by the drive, with  $|\psi_t\rangle$  the exact time-dependent state of the system.

Early numerical studies in Ref. [16] evidenced the lack of any KZM for the density  $\langle\nu_t\rangle$  of topological defects in the LMG model under the quasistatic drive across its QCP. As a matter of fact,  $\langle\nu_t\rangle$  shows universal behavior as a function of the combined variable  $N/\tau$ , where  $N$  is the size of the system and  $\tau$  is the drive rate. By choosing  $\omega_C \propto N^{-1/3}$  and  $\eta = 1$ , our effective model quite perfectly reproduces these exact numerical findings, as shown in Fig. 1 where we compare the irreversible work obtained by the effective model in Eq. (3) (upper panel) and the one found numerically in Ref. [16] for the LMG Hamiltonian (2) (lower panel).

*Full counting statistics of defects formation*—As it was recently shown for the nearest-neighbor Ising Hamiltonian, universality is not only observed in the scaling of the defects density, but in the entire full counting statistics of

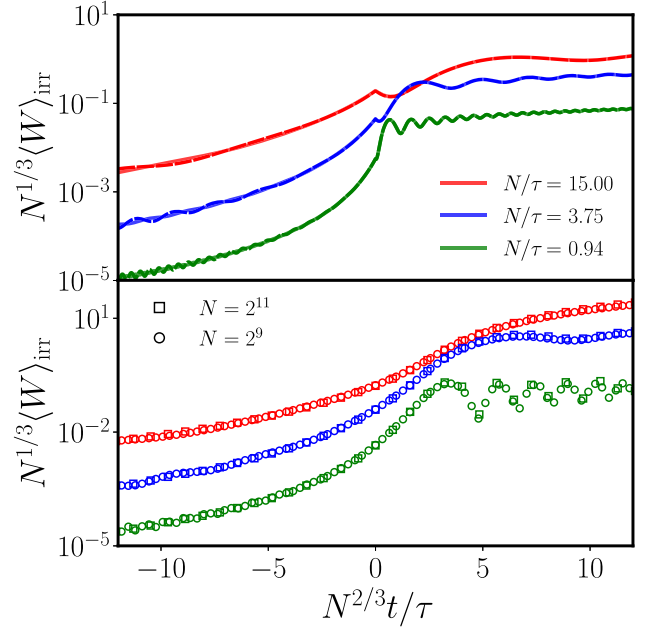


FIG. 1. Irreversible work associated respectively to the effective model in Eq. (3) (upper panel) and to the full numerical solution of the time-dependent LMG model in Eq. (2), with time-dependent coupling  $\lambda = t/\tau$ , performed in Ref. [16] (lower panel). Each color represents a different value of  $N/\tau$  (see legend), with  $N$  and  $\tau$  denoting the size of the system and drive rate respectively. Dashed and solid lines in the upper panel correspond to two system sizes,  $N = 2^9$  and  $N = 2^{11}$ , which are represented by different symbols for the numerical data (lower panel, see legend). Both the work and the time variables have been rescaled as described in Refs. [16,17]. The similarity between the theoretical model and the numerics demonstrates the capability of the effective model in Eq. (3) to describe the universal slow-drive dynamics of the LMG model in Eq. (2).

defects generated by the quasistatic drive [10,11]. Within our model (3), it is possible to derive the exact expression for the probability to generate a state with energy  $E_t^{(m)}$ ,

$$p(E_t^{(m)}) = \frac{(m-1)!!}{m!!} \sqrt{1 - |R_t|^2} |R_t|^m, \quad (6)$$

where  $m \in 2\mathbb{N}$  and

$$|R_t|^2 = \frac{\left(\frac{1}{2\xi_t^2} - \omega_t\right)^2 + \frac{\xi_t^2}{\xi_t^2}}{\left(\frac{1}{2\xi_t^2} + \omega_t\right)^2 + \frac{\xi_t^2}{\xi_t^2}}. \quad (7)$$

In Eq. (7),  $\xi_t$  denotes the time-dependent length of the oscillator, which obeys the Ermakov equation. From Eq. (6) one can derive the exact expression for all correlations of the defects density in terms of the coefficient  $|R_t|^2$  [41]. In particular, it is worth noting that

$$\langle\nu_t\rangle = \frac{|R_t|^2}{1 - |R_t|^2} \quad \text{and} \quad \langle\nu_t^2\rangle = \frac{|R_t|^2(2 + |R_t|^2)}{(1 - |R_t|^2)^2}, \quad (8)$$

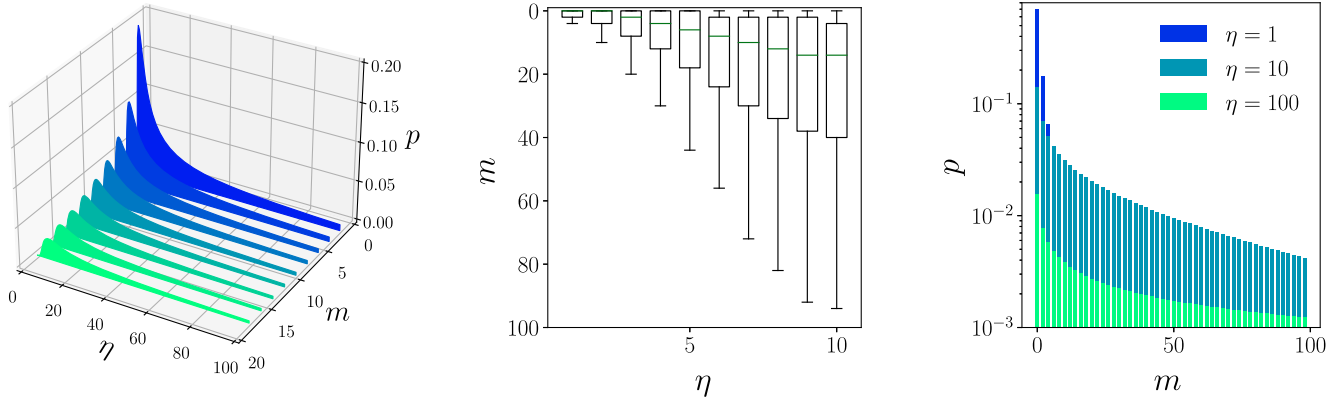


FIG. 2. Left: plot of the probability  $p(E_t^{(m)})$  in Eq. (6), as a function of  $\eta \in \mathbb{R}$  for different (even) values of  $m \in 2\mathbb{N}$  in the limit  $\tau \rightarrow \infty$ . As derived in the main text,  $p(E_t^{(m)})$  coincides with the probability of defects formation  $\mathcal{P}(m)$ , which behaves as a negative binomial distribution. Mid: top-down view of the distributions at fixed  $\eta$ . They are represented as a box plot with average value (green solid line), standard deviation (rectangular boxes), and domain (lower and upper extremes). Right: probability distributions at  $\eta = 1$ ,  $\eta = 10$ , and  $\eta = 100$ , respectively (in log scale). We can observe how the number of energy excitations, which are peaked around zero for small values of  $\eta$ , quickly spreads out to higher values of  $m$  as  $\eta$  increases.

which exclusively depend on  $\omega_t$  and  $\xi_t$  via  $|R_t|^2$ . All the cumulants of the full counting statistics of defects obey the same scaling theory observed for the average defect density in Fig. 1.

In the perfect quasistatic limit  $\tau \rightarrow \infty$ , the energy probability distribution coincides with the probability of defects formation after a perfect quantum annealing protocol:  $\lim_{\tau \rightarrow \infty} p(E_t^{(m)}) = \mathcal{P}(m)$ . We derived this from initializing the quantum system in the ground state. Interestingly, in this limit, one has an analytic expression for  $|R_t|$ , which reads

$$\lim_{\tau \rightarrow \infty} |R_t| = \cos\left(\frac{\pi}{2 + \eta}\right). \quad (9)$$

Thus, inserting the latter expression in Eq. (6), one obtains the exact expression of the probability for the formation of defects in a quantum LR ferromagnet after a slow quantum annealing procedure,

$$\mathcal{P}(m) = \binom{m/2 + r - 1}{m/2} \sin\left(\frac{\pi}{2 + \eta}\right)^{2r} \cos\left(\frac{\pi}{2 + \eta}\right)^m. \quad (10)$$

Equation (10) is a *negative binomial distribution* with a non-integer number of successes [52]. Indeed, from Eq. (6) it follows that  $r = 1/2$ . Because of the fractional value of  $r$ , the process of defects formation in LR quantum systems cannot be related to a classical combinatorial problem as it is the case for local quantum systems [14]. Equation (10) is the main result of the Letter.

The universal nature of the negative binomial distribution in Eq. (10) embodies two distinct features: (i) first, the probability distribution  $\mathcal{P}(m)$  only depends on the scaling variable  $N/\tau$  that makes the thermodynamic-limit result

independent, and thus universal, with respect to the ramp duration  $\tau$ . (ii) Since the distribution arises from the effective theory in Eq. (3), one may expect its applicability to extend to all those systems that share the same low-energy theory, namely a bosonic theory with gapped quasiparticle spectrum. Further theoretical and numerical investigation shall validate latter conjecture in ferromagnetic spin systems with generic strong LR interactions ( $\alpha < d$ ) [29]. The distribution is plotted in Fig. 2 as a function of both  $m \in 2\mathbb{N}$  (number of defects) and  $\eta$ . Greater is the value of  $\eta$ , and larger is the support of  $\mathcal{P}(m)$  along the  $m$  axis. So, both the average value and the variance of  $\nu_t$  increase monotonically as  $\eta$  increases; see the central panel in Fig. 2 and Eq. (8).

*Quantum thermodynamics at criticality*—We now consider the thermodynamic interpretation. While crossing the QCP at  $t = 0$ , a significant irreversible component of work is generated on average. In fact, as shown in Fig. 3, before  $t = 0$  the mean internal energy  $\langle \Delta E_t \rangle$  follows the time dependence imposed by the driving function  $\omega_t^2 = |t|$ , with  $\eta = 1$  in the figure. This entails  $\langle W \rangle_{\text{irr}} \approx 0$  for  $t < 0$ . Conversely, crossing the QCP makes irreversible the quantum system dynamics, and such irreversibility gets more pronounced as  $\omega_C$  decreases, with  $\omega_C$  quantifying the distance from perfect criticality. For  $\omega_C$  approaching zero, irreversible work is generated not only on average but also at the level of fluctuations. This is evident from the fact that  $\text{Var}(\Delta E_t)$ , variance of  $\Delta E_t$ , is proportional to  $\text{Var}(\nu_t)$  at any time  $t$ . From the distinction between reversible and irreversible work in Eq. (5) and Fig. 3,  $\text{Var}(\Delta E_t)$  has to be interpreted as the variance of the irreversible work for  $\omega_C \rightarrow 0$  [46].

Figure 3 demonstrates the irreversibility of the work process when the QCP is perfectly achieved for  $\omega_C = 0$ . In general, the *quantum adiabatic theorem* [53,54] guarantees

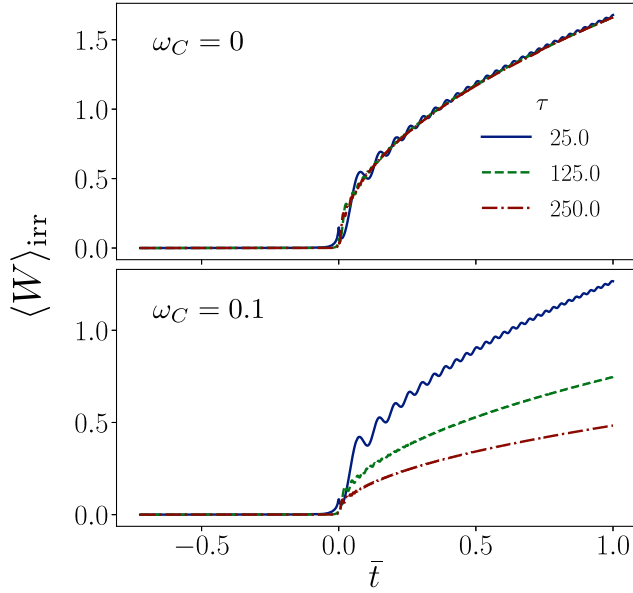


FIG. 3. Average irreversible work  $\langle W \rangle_{\text{irr}}$  as a function of the normalized time  $\bar{t} = t/\tau$  for different values of  $\tau$ . In the top panel we can observe that, for  $\omega_C \approx 0$ , increasing  $\tau$  does not help restore the adiabaticity of the system, and thus also  $\langle W \rangle_{\text{irr}}$  cannot be decreased. Instead, in the bottom panel, for a small (but finite)  $\omega_C = 0.1$  (in dimensionless units), it is possible to reduce the effect of irreversibility by increasing the time  $\tau$ , as predicted by the quantum adiabatic theorem [53,54].

that on average the internal energy of a driven quantum system tends to vanish in the limit of slow driving, i.e.,  $\tau \rightarrow \infty$ . For any  $\omega_C > 0$ , indeed, the internal energy of the system vanishes with a scaling depending on  $\tau$  [51]; see the lower panel in Fig. 3. Conversely, if  $\omega_C \rightarrow 0$  the quantum adiabatic theorem does not apply and the driving process is irreversible. As a consequence,  $\langle W \rangle_{\text{irr}}/(\hbar\omega_t) = \langle \nu_t \rangle$  is universal and independent of  $\tau$ .

**Conclusions**—In this Letter we answer the question about how the statistics of topological defects formation, the breaking of the quantum adiabatic theorem, and the production of energy excitations are linked to each other in quantum LR systems. LR couplings create strong correlations between traditional topological defects, causing them to lose their Fermi character. In the flat interaction limit, the low-energy theory simplifies to a single coherent state, like a condensate, which stays in its ground state at equilibrium. As the system nears the critical point, higher coherent states resonate with the ground state and become populated. Beyond the critical point, these high-energy modes become energetically separated from the ground state, preventing defect reabsorption and rendering the traditional KZM approach inapplicable.

Contrarily to local quantum systems [10–14], the finite time crossing of an infinitely degenerate QCP gives rise to energy excitations in the system dynamics that, in probability, follows a negative binomial distribution with a fractional number ( $r = \frac{1}{2}$ ) of “success” events (no defects).

These concepts are connected with the first law of thermodynamics in driven quantum systems. We have shown how to distinguish among the distributions of reversible and irreversible work while crossing an infinitely degenerate QCP, by providing an explanation in energetic terms of the corresponding adiabatic and nonadiabatic regimes. The latter are originated by the breaking of the quantum adiabatic theorem due to the spectral degeneracy at  $\omega_C = 0$ . In fact, until the QCP is not reached, the system can be driven adiabatically and the amount of irreversible work is negligible. Then, in correspondence of the criticality, any statistical moments of the internal energy distribution become nonanalytic, and immediately after, the dynamics becomes irreversible. This irreversibility originates from energy excitations, which are not reabsorbed in later dynamical stages, a universal feature expected in LR quantum systems with flat interactions ( $\alpha = 0$ ), where traditional Kibble-Zurek arguments fail [16,17].

Our predictions can be experimentally observed in various quantum platforms capable of fully connected interactions and complex geometries. Currently, trapped ion systems can achieve fully connected interactions with tunable power-law decay exponents in isolated environments [55]. Cold atoms trapped in optical cavities have been traditionally used to engineer flat interacting systems [56,57]. Additionally, Rydberg atom systems, already employed in investigating defect formation [58,59], are promising for observing our predictions due to their recent use in creating tunable complex geometries and custom interaction patterns [60]. Finally, it is worth noting that the definition of defects according to the Hamiltonian (3) is highly nonlocal and, therefore, connected to complex configurations of the original spin variables. In this perspective, experimental measurements could be rather directed to measure excitation energy statistics or the total excitation probability  $p_{\text{exc}} = 1 - \sqrt{1 - |R_t|^2}$ .

**Acknowledgments**—S. G. warmly thanks Ricardo Puebla for discussions about irreversible work generation from crossing an infinitely degenerate QCP. N. D. acknowledges useful discussion with G. M. Graf during the early stages of this work. This work was supported by The Blanceflor Foundation for financial support through the project “The theRmodynamics behInd thE meaSuremenT postulate of quantum mEchanics (TRIESTE),” European Union under GA No. 101077500–QLR-Net, the PNRR MUR project PE0000023–NQSTI funded by the European Union–Next Generation EU (N. D. and S. G.) and the PNRR MUR project SOE0000098 (L. B.). This research was funded in part by the Swiss National Science Foundation (SNSF) [200021\_207537]. The support of the Deutsche Forschungsgemeinschaft (DFG, German Research Foundation) under Germany’s Excellence Strategy EXC2181/1–390900948 (the Heidelberg STRUCTURES Excellence Cluster) is also acknowledged (N. D.).

- [1] T. W. B. Kibble, Topology of cosmic domains and strings, *J. Phys. A* **9**, 1387 (2001).
- [2] W. H. Zurek, Cosmological experiments in superfluid helium?, *Nature (London)* **317**, 505 (1985).
- [3] T. Kibble, Some implications of a cosmological phase transition, *Phys. Rep.* **67**, 183 (1980).
- [4] W. Zurek, Cosmological experiments in condensed matter systems, *Phys. Rep.* **276**, 177 (1996).
- [5] J. Dziarmaga, Dynamics of a quantum phase transition and relaxation to a steady state, *Adv. Phys.* **59**, 1063 (2010).
- [6] A. del Campo and W. H. Zurek, Universality of phase transition dynamics: Topological defects from symmetry breaking, *Int. J. Mod. Phys. A* **29**, 1430018 (2014).
- [7] T. Kibble, Phase-transition dynamics in the lab and the universe, *Phys. Today* **60**, No. 9, 47 (2007).
- [8] W. H. Zurek, U. Dorner, and P. Zoller, Dynamics of a quantum phase transition, *Phys. Rev. Lett.* **95**, 105701 (2005).
- [9] J. Dziarmaga, Dynamics of a quantum phase transition: Exact solution of the quantum Ising model, *Phys. Rev. Lett.* **95**, 245701 (2005).
- [10] A. del Campo, Universal statistics of topological defects formed in a quantum phase transition, *Phys. Rev. Lett.* **121**, 200601 (2018).
- [11] F. J. Gómez-Ruiz, J. J. Mayo, and A. del Campo, Full counting statistics of topological defects after crossing a phase transition, *Phys. Rev. Lett.* **124**, 240602 (2020).
- [12] J.-M. Cui, F. Gómez-Ruiz, Y.-F. Huang, C.-F. Li, G.-C. Guo, and A. del Campo, Experimentally testing quantum critical dynamics beyond the Kibble–Zurek mechanism, *Commun. Phys.* **3**, 44 (2020).
- [13] Y. Bando, Y. Susa, H. Oshiyama, N. Shibata, M. Ohzeki, F. J. Gómez-Ruiz, D. A. Lidar, S. Suzuki, A. del Campo, and H. Nishimori, Probing the universality of topological defect formation in a quantum annealer: Kibble-Zurek mechanism and beyond, *Phys. Rev. Res.* **2**, 033369 (2020).
- [14] S. Vishveshwara, Defect or no defect: It’s a toss up, *Physics* **13**, 98 (2020).
- [15] S. Sachdev, *Quantum Phase Transitions* (Cambridge University Press, Cambridge, England, 1999).
- [16] O. L. Acevedo, L. Quiroga, F. J. Rodríguez, and N. F. Johnson, New dynamical scaling universality for quantum networks across adiabatic quantum phase transitions, *Phys. Rev. Lett.* **112**, 030403 (2014).
- [17] N. Defenu, T. Enss, M. Kastner, and G. Morigi, Dynamical critical scaling of long-range interacting quantum magnets, *Phys. Rev. Lett.* **121**, 240403 (2018).
- [18] A. Solfanelli, G. Giachetti, M. Campisi, S. Ruffo, and N. Defenu, Quantum heat engine with long-range advantages, *New J. Phys.* **25**, 033030 (2023).
- [19] P. Jurcevic, B. P. Lanyon, P. Hauke, C. Hempel, P. Zoller, R. Blatt, and C. F. Roos, Quasiparticle engineering and entanglement propagation in a quantum many-body system, *Nature (London)* **511**, 202 (2014).
- [20] P. Hauke and L. Tagliacozzo, Spread of correlations in long-range interacting quantum systems, *Phys. Rev. Lett.* **111**, 207202 (2013).
- [21] J. Eisert, M. van den Worm, S. R. Manmana, and M. Kastner, Breakdown of quasilocality in long-range quantum lattice models, *Phys. Rev. Lett.* **111**, 260401 (2013).
- [22] P. Richerme, Z.-X. Gong, A. Lee, C. Senko, J. Smith, M. Foss-Feig, S. Michalakis, A. V. Gorshkov, and C. Monroe, Non-local propagation of correlations in quantum systems with long-range interactions, *Nature (London)* **511**, 198 (2014).
- [23] Z.-X. Gong, M. Foss-Feig, S. Michalakis, and A. V. Gorshkov, Persistence of locality in systems with power-law interactions, *Phys. Rev. Lett.* **113**, 030602 (2014).
- [24] L. F. Santos, F. Borgonovi, and G. L. Celardo, Cooperative shielding in many-body systems with long-range interaction, *Phys. Rev. Lett.* **116**, 250402 (2016).
- [25] Z.-X. Gong, M. Foss-Feig, F. G. S. L. Brandão, and A. V. Gorshkov, Entanglement area laws for long-range interacting systems, *Phys. Rev. Lett.* **119**, 050501 (2017).
- [26] A. Solfanelli, S. Ruffo, S. Succi, and N. Defenu, Logarithmic, fractal and volume-law entanglement in a Kitaev chain with long-range hopping and pairing, *J. High Energy Phys.* **05** (2023) 066.
- [27] M. Kastner, Diverging equilibration times in long-range quantum spin models, *Phys. Rev. Lett.* **106**, 130601 (2011).
- [28] T. Mori, T. N. Ikeda, E. Kaminishi, and M. Ueda, Thermalization and prethermalization in isolated quantum systems: A theoretical overview, *J. Phys. B* **51**, 112001 (2018).
- [29] N. Defenu, Metastability and discrete spectrum of long-range systems, *Proc. Natl. Acad. Sci. U.S.A.* **118**, e2101785118 (2021).
- [30] D. Jaschke, K. Maeda, J. D. Whalen, M. L. Wall, and L. D. Carr, Critical phenomena and Kibble–Zurek scaling in the long-range quantum Ising chain, *New J. Phys.* **19**, 033032 (2017).
- [31] N. Defenu, G. Morigi, L. Dell’Anna, and T. Enss, Universal dynamical scaling of long-range topological superconductors, *Phys. Rev. B* **100**, 184306 (2019).
- [32] Z. Fei, N. Freitas, V. Cavina, H. T. Quan, and M. Esposito, Work statistics across a quantum phase transition, *Phys. Rev. Lett.* **124**, 170603 (2020).
- [33] M. Singh, S. Dhara, and S. Gangadharaiah, Driven one-dimensional noisy Kitaev chain, *Phys. Rev. B* **107**, 014303 (2023).
- [34] H. J. Lipkin, N. Meshkov, and A. J. Glick, Validity of many-body approximation methods for a solvable model, *Nucl. Phys.* **62**, 188 (1965).
- [35] N. Meshkov, A. J. Glick, and H. J. Lipkin, Validity of many-body approximation methods for a solvable model. (II). Linearization procedures, *Nucl. Phys.* **62**, 199 (1965).
- [36] A. J. Glick, H. J. Lipkin, and N. Meshkov, Validity of many-body approximation methods for a solvable model. (III). Diagram summations, *Nucl. Phys.* **62**, 211 (1965).
- [37] V. Bapst and G. Semerjian, On quantum mean-field models and their quantum annealing, *J. Stat. Mech.* (2012) P06007.
- [38] T. Holstein and H. Primakoff, Field dependence of the intrinsic domain magnetization of a ferromagnet, *Phys. Rev.* **58**, 1098 (1940).
- [39] A. Rückriegel, A. Kreisel, and P. Kopietz, Time-dependent spin-wave theory, *Phys. Rev. B* **85**, 054422 (2012).
- [40] A. Lerose, J. Marino, B. Žunkovič, A. Gambassi, and A. Silva, Chaotic dynamical ferromagnetic phase induced by nonequilibrium quantum fluctuations, *Phys. Rev. Lett.* **120**, 130603 (2018).

- [41] See Supplemental Material at <http://link.aps.org/supplemental/10.1103/PhysRevLett.133.113401> for more details, which includes Ref. [42–49] and contains numerical evaluations of  $\text{Var}(\Delta E_t)$ .
- [42] S. Dusuel and J. Vidal, Continuous unitary transformations and finite-size scaling exponents in the Lipkin-Meshkov-Glick model, *Phys. Rev. B* **71**, 224420 (2005).
- [43] R. Dabrowski and G. V. Dunne, Time dependence of adiabatic particle number, *Phys. Rev. D* **94**, 065005 (2016).
- [44] H. R. Lewis, Classical and quantum systems with time-dependent harmonic-oscillator-type Hamiltonians, *Phys. Rev. Lett.* **18**, 510 (1967).
- [45] H. R. Lewis Jr. and W. B. Riesenfeld, An exact quantum theory of the time-dependent harmonic oscillator and of a charged particle in a time-dependent electromagnetic field, *J. Math. Phys. (N.Y.)* **10**, 1458 (1969).
- [46] S. Gherardini, A. Belenchia, M. Paternostro, and A. Trombettoni, End-point measurement approach to assess quantum coherence in energy fluctuations, *Phys. Rev. A* **104**, L050203 (2021).
- [47] S. Hernández-Gómez, S. Gherardini, A. Belenchia, A. Trombettoni, M. Paternostro, and F. N., Experimental signature of initial quantum coherence on entropy production, *npj Quantum Inf.* **9**, 86 (2023).
- [48] P. Talkner, E. Lutz, and P. Hänggi, Fluctuation theorems: Work is not an observable, *Phys. Rev. E* **75**, 050102(R) (2007).
- [49] M. Campisi, P. Hänggi, and P. Talkner, Colloquium: Quantum fluctuation relations: Foundations and applications, *Rev. Mod. Phys.* **83**, 771 (2011).
- [50] N. Defenu, Quantum adiabatic cycles and their breakdown: An analytic solution, *Commun. Phys.* **4**, 150 (2021).
- [51] S. Deffner and E. Lutz, Nonequilibrium work distribution of a quantum harmonic oscillator, *Phys. Rev. E* **77**, 021128 (2008).
- [52] M. H. Degroot, *Probability and Statistics*, 2nd ed. (Addison Wesley Publishing Company, Boston, 1986).
- [53] L. D. Landau and E. M. Lifshitz, *Statistical Physics. Pt. I* (Butterworth-Heinemann, London, 1969).
- [54] T. Kato, On the adiabatic theorem of quantum mechanics, *J. Phys. Soc. Jpn.* **5**, 435 (1950).
- [55] C. Monroe, W. C. Campbell, L.-M. Duan, Z.-X. Gong, A. V. Gorshkov, P. W. Hess, R. Islam, K. Kim, N. M. Linke, G. Pagano, P. Richerme, C. Senko, and N. Y. Yao, Programmable quantum simulations of spin systems with trapped ions, *Rev. Mod. Phys.* **93**, 025001 (2021).
- [56] F. Mivehvar, F. Piazza, T. Donner, and H. Ritsch, Cavity QED with quantum gases: New paradigms in many-body physics, *Adv. Phys.* **70**, 1 (2021).
- [57] N. Defenu, T. Donner, T. Macrì, G. Pagano, S. Ruffo, and A. Trombettoni, Long-range interacting quantum systems, *Rev. Mod. Phys.* **95**, 035002 (2023).
- [58] A. Keesling, A. Omran, H. Levine, H. Bernien, H. Pichler, S. Choi, R. Samajdar, S. Schwartz, P. Silvi, S. Sachdev, P. Zoller, M. Endres, M. Greiner, V. Vuletić, and M. D. Lukin, Quantum Kibble–Zurek mechanism and critical dynamics on a programmable Rydberg simulator, *Nature (London)* **568**, 207 (2019).
- [59] L. Chomaz, I. Ferrier-Barbut, F. Ferlaino, B. Laburthe-Tolra, B. L. Lev, and T. Pfau, Dipolar physics: A review of experiments with magnetic quantum gases, *Rep. Prog. Phys.* **86**, 026401 (2022).
- [60] A. Periwal, E. S. Cooper, P. Kunkel, J. F. Wienand, E. J. Davis, and M. Schleier-Smith, Programmable interactions and emergent geometry in an array of atom clouds, *Nature (London)* **600**, 630 (2021).